Silicon (2018) 10:1819–1829
https://doi.org/10.1007/s12633-017-9675-1

ORIGINAL PAPER

Dry Sliding Friction and Wear Behavior of AA7075-Si_3N_4 Composite

Mir Irfan Ul Haq[1] · **Ankush Anand**[1]

Received: 25 May 2017 / Accepted: 2 November 2017 / Published online: 14 March 2018
© Springer Science+Business Media B.V., part of Springer Nature 2018

Abstract The present investigation is aimed at identifying the influence of Si_3N_4 reinforcement on the mechanical and tribological behavior of AA7075-Si_3N_4 composite. Five different composites of AA7075 aluminum alloy reinforced by silicon nitride particles have been fabricated by the stir casting route. The percentage of silicon nitride was varied from 0-8 wt%. The cast composites were tested for hardness, density and compression strength. Unidirectional friction and wear testing was carried out for all compositions under five different loading conditions (10 N, 20 N, 30 N, 40 N and 50 N) at a constant sliding speed of 1 m/s. SEM and EDS analysis was also carried out for worn surface analysis and elemental analysis of the composites. The hardness and compression strength of the composites exhibited an increasing trend with an increase in wt% of reinforcement in the base alloy, showing 20% improvement in hardness and around 50% improvement in compression strength for 8 wt% Si_3N_4 addition. The addition of Si_3N_4 particles led to an improvement in the wear resistance by 37% at low loads (10 N) and 61% at higher loads (50 N). The COF for all varied compositions at low load (10 N) and high load (50 N) ranges from 0.10 to 0.20 and 0.25 to 0.30 respectively. Moreover, the COF is observed to increase until 4 wt% and beyond it decreases. Microscopic studies of worn surfaces revealed a dominance of delamination wear at lower concentrations (0 wt% and 2 wt%) and ploughing at higher concentrations (6 wt% and 8 wt%). The developed composites exhibited better mechanical and anti-wear properties and could serve as potential candidates in sliding applications such as bearings, brake drums, gears, sprockets and brake rotors.

Keywords Metal matrix composite · Wear · Friction · Stir casting

1 Introduction

The growing environmental concerns and quest for improved fuel efficiency has forced researchers to work towards development of sustainable materials [1]. The widespread involvement of friction and wear in engineering applications has caused tribologists and material scientists to work towards exploring new materials with better mechanical and tribological properties. Aluminum alloys owing to their high strength to weight ratio find wide applications in engineering components, more specifically in the automotive and aerospace industry [2–4]. Characteristics like good corrosion resistance, low electrical resistivity, ease of machining, high damping capacity and relatively low cost further widen their scope for a large number of engineering applications [5, 6]. The major issue associated with the use of aluminum alloys is their low wear resistance under dry, starved and lubricated conditions [7]. In order to improve their mechanical and tribological properties, various reinforcing agents like alumina (Al_2O_3), silicon carbide (SiC), boron carbide (B_4C), etc. have been tried during the past decade with various aluminum alloys to develop aluminum matrix composites (AMCs). The reinforcement is either done in the solid state (e.g. powder metallurgy) or in the liquid state. The liquid state methods like stir casting, spray casting and squeeze casting have been widely used in the case of AMCs due to their technical and economic benefits involved in the production of large sized parts [8, 9].

✉ Ankush Anand
anand.ankush13@gmail.com

[1] Department of Mechanical Engineering, Shri Mata Vaishno Devi University, Katra, Jammu and Kashmir, 182320, India

Table 1 Chemical composition of AA7075 aluminum alloy

Elements	Zn	Mg	Cu	Mn	Fe	Cr	Ti	Si	Al
Weight%	5.8	2.4	1.4	0.04	0.18	0.18	0.06	0.07	Remaining

In order to improve the structural performance of pure aluminum, various alloying elements are added resulting in aluminum alloys. AA7075 is a high strength aluminum alloy with zinc as the main alloying element. AA7075 exhibits highest strength as far as aluminum alloys are concerned and in many cases, the properties surpass high tensile steels [10, 11]. The strength of AA7075 is comparable to many steels, and has better fatigue strength and is widely used in marine, automotive and, aerospace industries [12]. However, owing to its low hardness and high susceptibility to adhesive wear, it exhibits poor tribological properties [13].

Various researchers have previously investigated bare AA7075 alloy for its tribological characteristics under different conditions of load, speed and, temperature [14–16]. Ceramic reinforcements like alumina, zirconia and silicon carbide are the most preferred reinforcements for improving the strength, hardness, wear resistance, corrosion resistance and high temperature performance. Kumar et al. [17] studied the effect of SiC on AA7075 and observed an improvement in density, hardness and tensile strength with the SiC addition. A similar investigation carried out by Laksmipathy and Kulendran [18] documented a significant improvement in wear resistance with the addition of SiC particles in AA7075. Daoud et al. [19] investigated the effect of Al_2O_3 on mechanical and wear behaviour of AA7075 alloy and the study revealed an increase in the hardness and wear resistance with an increase in the volume fraction of Al_2O_3 particles in comparison to the unreinforced alloy. Rajan et al. [2] studied the effect of TiB_2 on the AA7075, wherein it was observed that increased TiB_2 content led to higher wear resistance. Baradeswaran and Perumal [20] investigated the effect of B_4C on AA7075 and reported an improvement in hardness with an increase in volume fraction of particulates. Moreover, the wear rate as reported was considerably less compared to the pure matrix material. Baskaran et al. [21] in their study on AA7075-TiC composites observed decreased wear rate with the addition of TiC particles.

Based on the literature above, it can be inferred that the wear resistance and hardness of the AA7075 alloy improve considerably by the addition of ceramic particles (i.e. by making AA7075 composites).

Silicon nitride is an excellent tribological material used extensively in roller and ball bearings [22]. The characteristics like high mechanical strength, low density, lower friction, good thermal stability, low contact fatigue rates and better wear resistance [23] associated with silicon nitride (Si_3N_4) have not been explored much in the production of AMCs. Xiu et al. [24] have however, in their study related to Al/Si_3N_4 composites, reported an improved strength. Various researchers have reported an improvement in the hardness and wear resistance in the Si_3N_4 reinforced composites in comparison to the unreinforced alloys [25–28]. The literature reveals that Si_3N_4 being a good bearing material, unlike other reinforcing agents, has not been explored much. Moreover, much less data is available explaining the tribological properties of the composites with Si_3N_4 as the reinforcing agent.

In the present work, a novel composite comprising of AA7075 as the base matrix and Si_3N_4 as the reinforcement has been fabricated by using the stir casting route. Si_3N_4 is added in varying percentages by weight and the developed composites subjected to various mechanical and tribological tests. The aim of this work is to augment the good mechanical properties of AA7075 with the favourable tribological properties of silicon nitride, and thereby develop a composite that could serve various anti-wear and anti-friction engineering applications.

2 Materials and Methods

2.1 Fabrication of Composites

In the present investigation, AA7075 aluminum alloy procured from Bharat Aerospace Metals (Mumbai, India) was used as a base matrix. The chemical composition of the base matrix is provided in Table 1. Si_3N_4 supplied by Nanopartech Ltd. (Chandigarh, India) was used as the reinforcement material. The properties of the Si_3N_4 powder are presented in Table 2.

The silicon nitride (Si_3N_4) reinforcement was varied from (0–8)% by weight. The range of the reinforcement was finalized on the basis of previous literature [26, 29]. The details of the samples are given in Table 3. The stir casting route was used for fabrication of the composites. Aluminum alloy AA7075 of 500 g was heated to 950 °C in a graphite crucible in an electric furnace. Prior to reinforcement addition, dross was removed manually from the

Table 2 Properties of Si_3N_4 powder

Appearance	Purity	Oxygen content	Crystallographic form	Average particle size	Density	Morphology
Grey white powder	> 99%	> 0.61%	Cubic	> 40 μm	3.52 g/cm^3	Nearly spherical

Table 3 Details of samples

S.No.	AA 7075 (wt%)	Si_3N_4(wt%)
1	100	0
2	98	2
3	96	4
4	94	6
5	92	8

crucible. Preheated ceramic particles were added to the molten metal at a constant feed rate and mechanical stirring was carried out to ensure homogenous mixing of the ceramic particles [30]. The various process parameters are presented in Table 4. The composite was poured into a preheated permanent mold and thereafter allowed to cool at room temperature. The fabricated composites are presented in Fig. 1. The cast samples were then machined to form cylindrical pins of required dimensions as per the testing procedures. The presence of Si_3N_4 and its uniform distribution was confirmed by EDS and SEM respectively.

2.2 Mechanical Testing of Composites

The hardness, density and, compression strength of the cast samples were investigated. Archimedes' principle was used to measure the density of the composites. The micro-hardness measurement was carried out using a Vickers hardness tester according to ASTM E92 standard. The indentation load for every test was 5 N with a constant dwell time of 5 seconds. Micro-hardness of each composition was measured at five different locations and three samples per composition were tested to ensure repeatability of the results. The compression testing was carried out on samples with 10 mm diameter and 15 mm height (L/D ratio = 1.5) on a universal testing machine with constant velocity according to ASTM E9 standard. The compression testing for every composition was performed three times to ensure repeatability.

2.3 Tribological Testing of Composites

The tribological studies were carried out on a computer integrated pin-on-disc tribometer (DUCOM Wear and Friction Monitor TR-20LE-PHM400) with an inbuilt load cell to measure the frictional force (Fig. 2).

Table 4 Process parameters used in stir casting

S. No.	Parameter	Value
1	Stirring temperature	950 °C
2	Stirring RPM	250 RPM
3	Stirring time	10 min
4	Preheat temperature of Si_3N_4 particles	450 °C
5	Preheat temperature of the permanent mold	300 °C

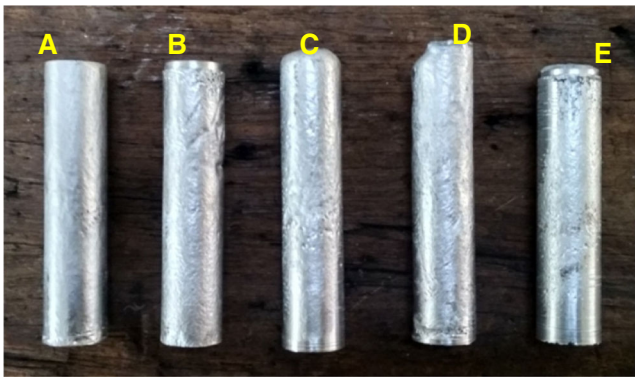

Fig. 1 Photograph of the cast composites with A) 0 wt% Si_3N_4 B) 2 wt% Si_3N_4 C) 6 wt% Si_3N_4 D) 4 wt% Si_3N_4 E) 8 wt% Si_3N_4

Cylindrical pins of the cast composites with 8 mm diameter and 8 mm height were used for tribological testing. A steel disc of EN 31 steel with a hardness value of around 60±3 HRC was used as the counterface material. The tribo-testing was carried out at five different normal loads (10 N, 20 N, 30 N, 40 N and 50 N). The sliding was carried up to a distance of 1500 m at a constant sliding speed of 1 m/s. The tribological testing was carried out at room temperature. Prior to every test, polishing of the samples was performed by different grades of silicon carbide emery papers to ensure similar surface roughness conditions (R_a value of around 0.03 μm). Acetone cleaned samples were

Fig. 2 Photograph of the pin-on-disc tribometer

Table 5 Experimental density of the cast composites

Si_3N_4 Content (wt %)	0	2	4	6	8
Experimental Density(g/cm^3)	2.78	2.80	2.83	2.87	2.90
Void Fraction	0.02	0.02	0.01	0.01	0.001

weighed by using an electronic weighing balance of accuracy 10^{-3} g. The wear loss was reported as a difference in weight of the samples measured before and after each test. Each experiment was repeated thrice and an average value is reported. Scanning electron microscopy (SEM) and EDS analysis were performed to analyse the worn surfaces and elemental analysis respectively.

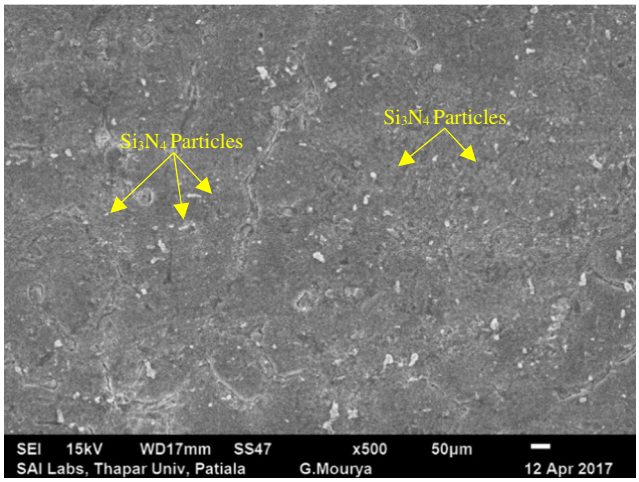

Fig. 4 Representative SEM image confirming uniform distribution of Si_3N_4 particles

3 Results and Discussions

3.1 Physical and Microstructural Properties

The experimental density of the cast samples is presented in Table 5. From the observations it is found that the density of the samples shows a slightly increasing trend with an increase in the reinforcement of the Si_3N_4 particles. Moreover, the void fraction for all the fabricated composites has been calculated and is indicated in Table 5. The density results are similar to the observations reported in an earlier study carried out by Sharma et al. [31]. This slight increase may be due to the higher density of the Si_3N_4 particles (3.52 g/cm^3) in comparison to the base alloy.

The presence of Si_3N_4 particles is confirmed by EDS images as shown in Fig. 3 and homogenous mixing of Si_3N_4 particles was confirmed by SEM (Fig. 4) wherein, it can be

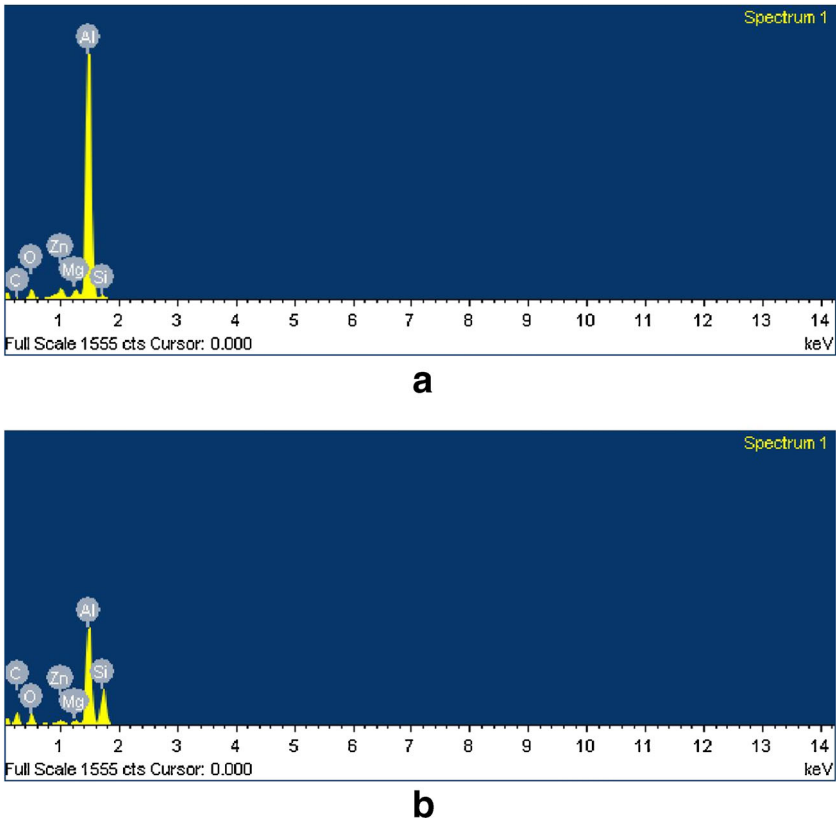

Fig. 3 EDS images of **a** AA7075 as cast alloy **b** AA7075 – 6 wt% cast composite

clearly seen that ceramic particles are evenly distributed in the matrix.

3.2 Mechanical Testing

3.2.1 Hardness

The variation in micro-hardness with an increase in the reinforcement material is shown in Fig. 5. The micro-hardness shows an increasing trend with the increase in the reinforcement. This improvement in the hardness may be ascribed to the increased ratio of the comparatively harder reinforcement in the matrix. Moreover, in hardness testing a concentrated load is applied on a localized region and in the case of the particle reinforced composite the density of the particles just below the indentation zone increases. This increase in the density of the hard ceramic particles in the localized zone of indentation, improves the hardness [32]. Also, the hard ceramic particles in the matrix act as load bearing elements and thus constrain the dislocation. A similar behavior in the hardness with the addition of reinforcement has been reported in earlier investigations [17, 33–35]. The microstructure of the cast composites as shown in Fig. 6 also revealed grain refinement with the increased content of the Si_3N_4 reinforcement. The grain refinement could help in improving the hardness. Mabuchi et al. have also documented that hard Si_3N_4 particle reinforcement acts as the driving force for the grain refinement [36].

3.2.2 Compression Strength

The variation of compression strength with an increase in the reinforcement is shown in Fig. 7. This variation shows a linear trend and can be attributed to the load bearing capacity of the composites which increased with the addition of Si_3N_4 particles. The hard ceramic particles restrict the dislocation and thus stop the crack propagation by deflecting the growth plane of the cracks. Also, the hard ceramic particles offer resistance to plastic flow, thereby improving the compression strength [20]. Similar variation in the compression strength with the addition of ceramic reinforcement has been reported by Suresh et al. [37]. The homogenous distribution (Fig. 4) of the ceramic particles in the matrix phase also improves the compression strength [38]. The observed grain refinement (Fig. 6) with the addition of the ceramic phase is also a contributing factor for the improved compression strength [39]. In addition to the aforementioned factors, the decreased distance between the particles upon

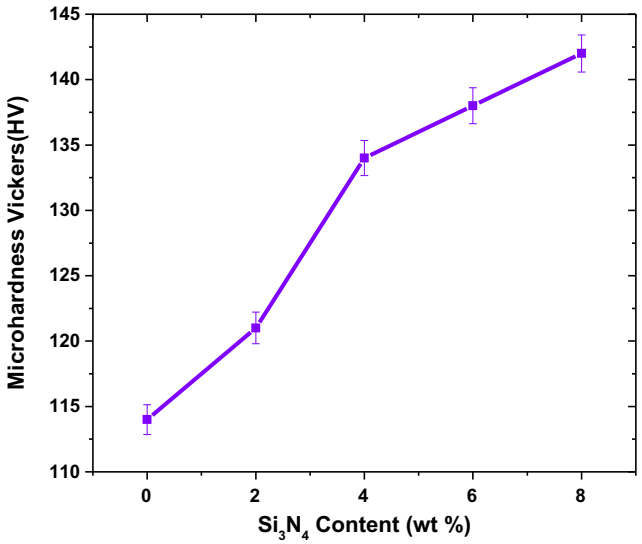

Fig. 5 Variation in hardness with increase in Si_3N_4 content

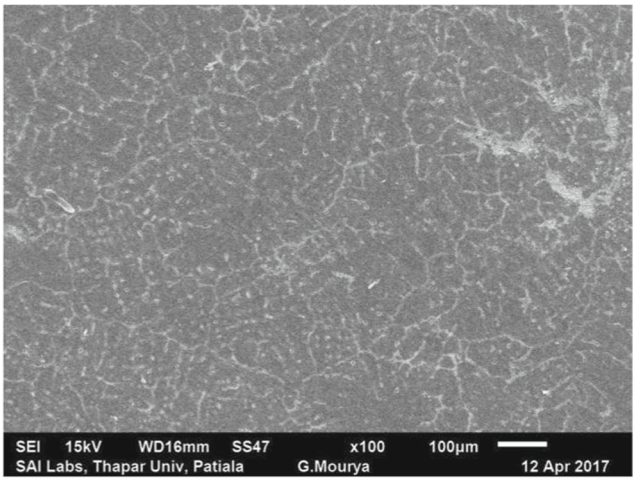

Fig. 6 Representative image of microstructure **a** 0 wt% Si_3N_4 **b** 8 wt% Si_3N_4

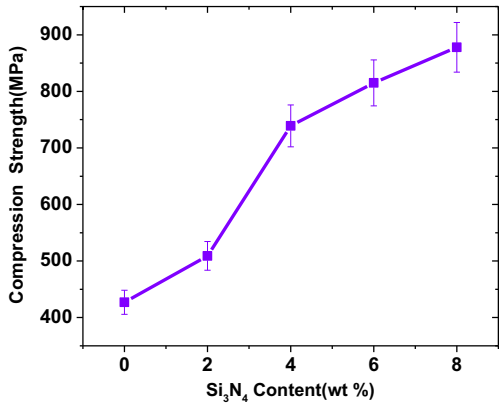

Fig. 7 Variation in compression strength with increase in Si_3N_4 content

the increase in the ceramic content leads to an improved strength [40].

3.3 Tribological Characteristics

3.3.1 Effect of Reinforcement on Wear

The variation of wear loss of the composites at different loads is shown in Fig. 8. As is evident from the figure, the wear resistance of composites improved with the addition of ceramic reinforcement at all loading conditions. A similar trend is observed in the wear behavior at every load. The wear resistance for 8 wt% Si_3N_4 reinforced composite improved by 37% at low loads (10 N) and around 61% at higher loads (50 N). The improvement in wear resistance may be attributed to the hardness of the composites which

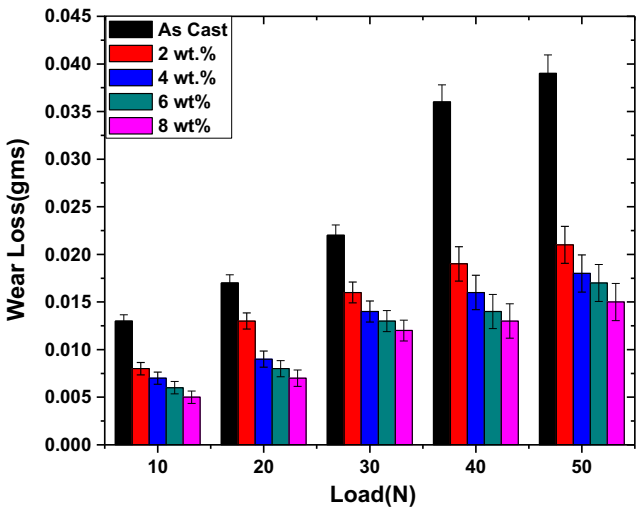

Fig. 8 Variation of wear loss for fabricated composites at different loads

increased with an increase in the reinforcement [41]. Moreover, with an increase in the concentration, the matrix area in contact with the counterface also reduces. The relatively softer unreinforced alloy undergoes higher plastic deformation thereby leading to increased wear loss [20]. Moreover, the hard ceramic particles resist the crack propagation and reduce the chances of material removal during the sliding process [2]. The grain refinement as revealed in the microstructure also results in improvement of wear resistance [42]. Furthermore, the SEM morphologies of the worn samples (Fig. 11) also revealed a shift from delamination wear towards abrasive wear mechanism as the reinforcement content increased. This shift in the wear mechanism also contributes to the decreased wear loss [43].

3.3.2 Effect of Load on Wear

It is evident from Fig. 8 that wear loss for all compositions increases with an increase in load which is in line with Archard's wear law [44], which states that the wear loss has a linear relationship with the normal load. However, the increase in wear loss is comparatively less for the reinforced composites in comparison to the base alloy. The higher loads leading to delamination, in turn resulting in higher wear loss may be the contributing factor for this behavior [41]. The increased material removal with increase in load can also be attributed to the penetration of hard asperities of the counterface into the softer pin surface [45]. Moreover, increase in temperature at higher loads also contributes to the increase in the wear loss [20].

3.3.3 Coefficient of Friction (COF)

The friction curves of all composites at loads of 10 N and 50 N are presented in Fig. 9. The coefficient of friction for all compositions at 10 N shows an increasing trend with an increase in sliding distance which may be attributed to an increase in the real area of contact. The sharp peaks observed in the friction curves at 10 N may be due to third body abrasion caused by wear debris. The COF in the case of lower load stabilized almost after 200 m as against 100 m in the case of higher loads. Nuruzzaman et al. [46] also reported a similar trend. The composition with 4 wt% Si_3N_4 exhibits highest COF both at 10 N and 50 N. An increase in COF for unreinforced alloy can be seen at 50 N load after 1000 m. This increase can be attributed to the breaking of asperities, as the ceramic particles which act as load bearing elements are absent, thereby leading to an increase in the real area of contact. The COF for all composites at 10 N and 50 N load ranges from 0.10 to 0.20 and 0.25 to 0.30 respectively.

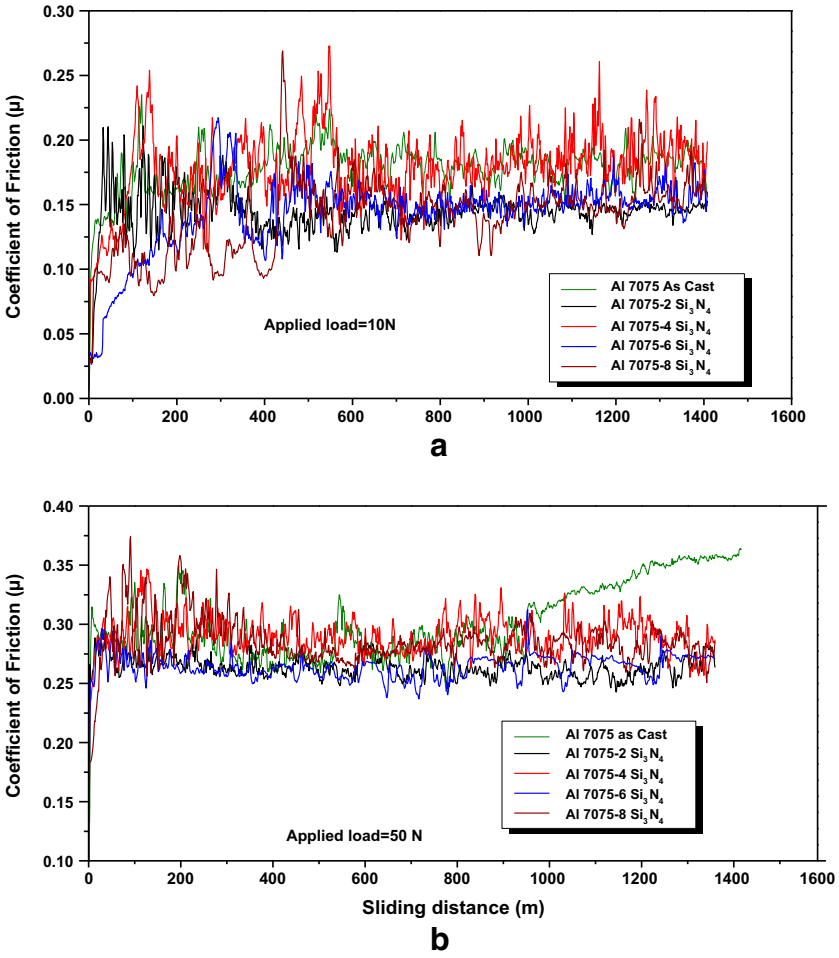

Fig. 9 Friction curves at **a** 10 N applied load **b** 50 N applied load

3.3.4 Effect of Reinforcement on COF

The variation of coefficient of friction (COF) with addition of Si_3N_4 is shown in Fig. 10. The COF increases with an increase in the concentration of Si_3N_4 up to 4 wt%, however, it decreases further with an increase in the reinforcement. A similar pattern is observed at all test loads. The increase in COF up to 4 wt% can be attributed to the delamination taking place at the interface (Fig. 11b). It may be noted that a transition in the wear mechanism from delamination to ploughing is clearly visible at 4 wt%. Moreover, the delamination mechanism observed at lower concentrations led to an increase in the COF [47] (Fig. 11). Hassan et al. [48] have also reported a similar behavior. The decreasing trend observed after 4 wt% may be ascribed to the increased content of the spherical shaped Si_3N_4 particles in the wear debris, resulting in the rolling contact at the interface [49].

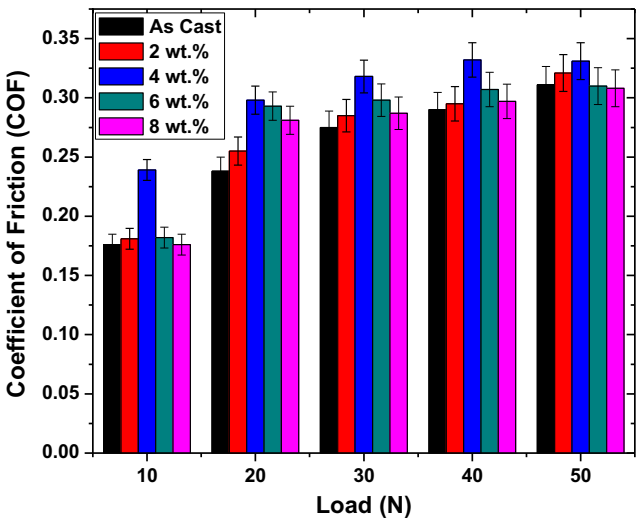

Fig. 10 Coefficient of friction variation for fabricated composites at different loads

3.3.5 Effect of Load on COF

The increase in load at the tribo-contact led to a linear increase in the COF for all concentrations (Fig. 10). This increase in the coefficient of friction may be attributed to the increased asperity contact at the interface. At lower loads (10 N and 20 N) the increase in the COF with load is considerable in comparison to the variation at higher loads

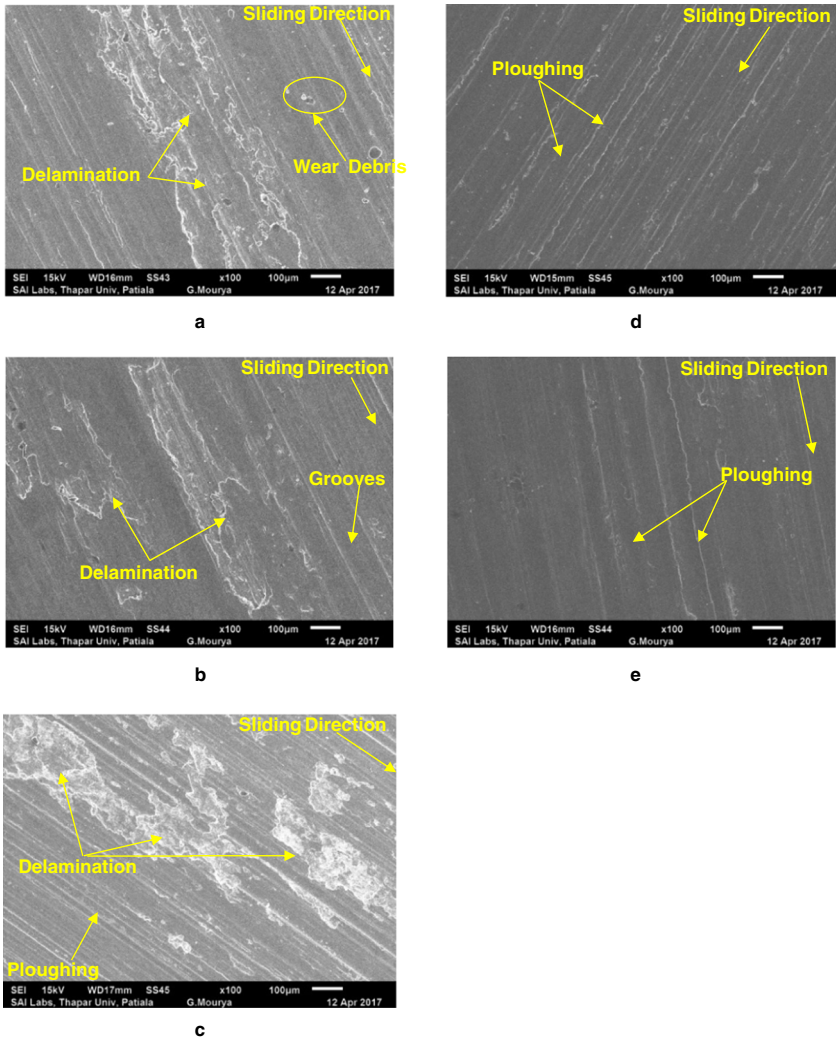

Fig. 11 SEM images of worn samples at 30 N load of **a** 0 wt% Si_3N_4 **b** 2 wt% Si_3N_4 **c** 4 wt% Si_3N_4 **d** 6 wt% Si_3N_4 **e** 8 wt% Si_3N_4

(40 N and 50 N). A similar behavior has been observed by Venkataraman and Sundararajan [50]. It can be concluded that the COF increases with an increase in the normal load. However, beyond a certain load, the COF becomes almost independent of load. Earlier literature also reports similar trends [46, 51].

3.4 Worn Surface Analysis

The SEM topographies of the worn samples revealed distinct wear mechanisms for different concentrations of Si_3N_4. In the case of the base composition (Fig. 11a), the prominent wear mechanisms are adhesion and delamination. However, slight ploughing can also be observed. A heavy plastic deformation can also be observed along the direction of the sliding, indicating higher wear loss. A similar morphology can be observed for 2 wt% Si_3N_4 composition (Fig. 11b). However, the adhesion and delamination mechanisms appear to be lesser in comparison to the base composition. For the composition with 4 wt% Si_3N_4, delamination wear is the dominant wear mechanism, in addition to the surface damage in the form of decohesion that can be observed (Fig. 11c). The SEM image (Fig. 12)

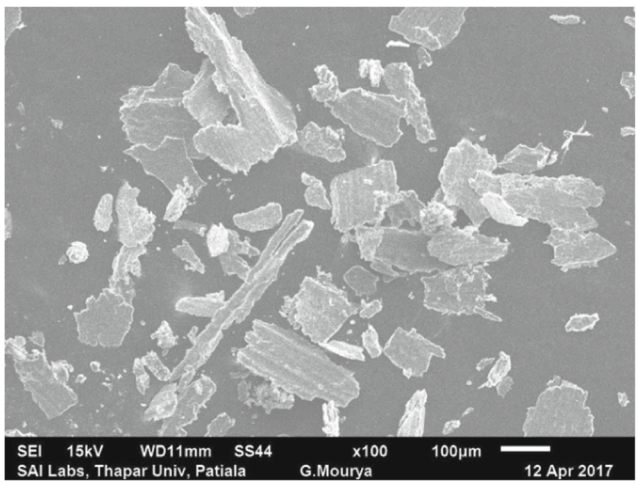

Fig. 12 SEM image of wear debris (4 wt% Si_3N_4)

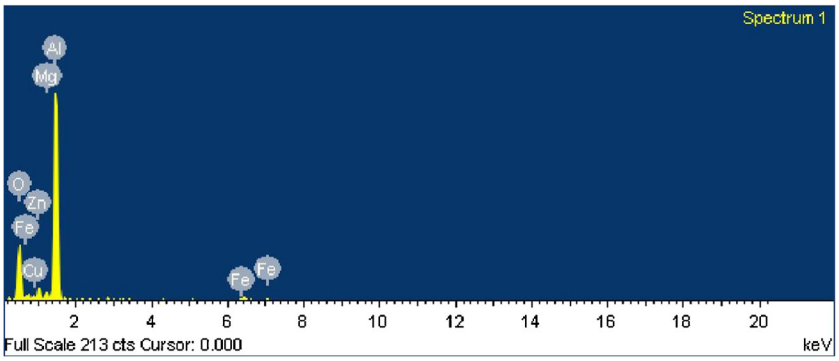

Fig. 13 EDS image of worn sample

of the wear debris for 4 wt% Si_3N_4 also revealed flake shaped debris which further suggests that delamination is the dominant wear mechanism [52]. With the increased content of Si_3N_4, the dominant abrasive wear mechanism in the form of ploughing can be clearly seen, wherein the delamination mechanism is almost absent (Fig. 11d and e). The shift in wear mechanism from delamination wear to abrasive wear with increase in reinforcement content is also reported in earlier literature [53]. A significant decrease in the plastic deformation is also observed which may be attributed to the hard ceramic particles. The EDS image of the worn surface presented in Fig. 13 also confirms the formation of a mechanically mixed layer (MML). The presence of iron (Fe) in the EDS image indicates the transfer of iron (Fe) from the counterbody. The penetration of wear debris into the grooves of the softer pin and, thereafter becoming engraved into the pin leads to the formation of the MML. The presence of reinforcement particles also aids in the formation of the MML [54]. The MML formation also contributes in improving the wear resistance of the composites [50].

4 Conclusions

1. An AA7075-Si_3N_4 composite have been successfully fabricated by using the stir casting route. The presence of ceramic particles and the homogenous mixing of ceramic particles in the matrix was confirmed by EDS and SEM respectively.
2. A 25% increase in the microhardness of the composites was observed on increasing the concentration of Si_3N_4 particles, which may be ascribed to the increase in the hard ceramic phase.
3. The compression strength also improved substantially (110%) on increasing the concentration of Si_3N_4 particles which may be attributed to the high load bearing capacity of the hard ceramic reinforcement.
4. A substantial improvement of 37% at low loads (10 N) and around 61% at higher loads (50 N) in the wear resistance was observed with the increase in the Si_3N_4 particles. Moreover, an increase in wear was observed with an increase in the normal load.
5. The coefficient of friction increased until 4 wt% composite and thereafter it decreased. At lower loads, the COF increased with an increase in load. However, beyond 30 N, COF is almost independent of load.
6. The wear mechanisms observed in the SEM images of the worn samples indicate a shift from a delamination at lower concentrations to abrasion in the form of ploughing at higher concentrations. The EDS of the worn surfaces confirmed the formation of a mechanically mixed layer (MML).
7. The developed composites could serve as potential candidate materials for antiwear and antifriction applications such as bearings, brake drums, gears, sprockets and brake rotors.

Acknowledgements The authors would like to acknowledge the help rendered by the staff of Central Workshop SMVDU. Moreover the financial assistance offered by SMVD University for carrying out the testing is also acknowledged. The authors would also like to thank SAI Labs Patiala, Punjab, India for extending their testing facility (SEM and EDS) in carrying out the testing.

References

1. Mohanty A, Misra M, Drzal L (2002) Sustainable bio-composites from renewable resources: opportunities and challenges in the green materials world. J Polym Environ 10:19–26
2. Rajan HM, Ramabalan S, Dinaharan I, Vijay S (2014) Effect of TiB 2 content and temperature on sliding wear behavior of AA7075/tib 2 in situ aluminum cast composites. Arch Civ Mech Eng 14:72–79
3. Poria S, Sahoo P, Sutradhar G (2016) Tribological characterization of stir-cast aluminium-TiB2. Silicon 8:591–599
4. Rao R, Das S (2011) Effect of applied pressure on the tribological behaviour of SiCp reinforced AA2024 alloy. Tribol Int 44:454–462
5. Singh N, Mir IUH, Raina A, Anand A, Kumar V, Sharma SM (2017) Synthesis and tribological investigation of Al-SiC based nano hybrid composite. AEJ(Article in Press). https://doi.org/10.1016/j.aej.2017.05.008
6. Singh S, Pal K (2015) Effect of surface modified silicon carbide particles with Al 2 O 3 and nanocrystalline spinel ZnAl 2 O 4 on

mechanical and damping properties of the composite. Mat Sci Eng A-Struct 644:325–336
7. Veeravalli RR, Nallu R, Mohiuddin SMM (2016) Mechanical and tribological properties of AA7075–tic metal matrix composites under heat treated (T 6) and cast conditions. J Mater Res Technol 5:377–383
8. Sajjadi SA, Ezatpour H, Beygi H (2011) Microstructure and mechanical properties of Al–Al 2 O 3 micro and nano composites fabricated by stir casting. Mat Sci Eng A-Struct 528: 8765–8771
9. Omrani E, Moghadam AD, Menezes PL, Rohatgi PK (2016) Influences of graphite reinforcement on the tribological properties of self-lubricating aluminum matrix composites for green tribology, sustainability, and energy efficiency—a review. Int J Adv Manuf Tech 83:325–346
10. Liu D, Atkinson H, Kapranos P, Jirattiticharoean W, Jones H (2003) Microstructural evolution and tensile mechanical properties of thixoformed high performance aluminium alloys. Mater Sci Eng A 361:213–224
11. Andreatta F, Terryn H, De Wit J (2004) Corrosion behaviour of different tempers of AA7075 aluminium alloy. Electrochim Acta 49:2851–2862
12. Kaufman JG (1999) Properties of aluminum alloys: tensile, creep, and fatigue data at high and low temperatures. ASM International
13. Liu Y, Mol J, Janssen G (2016) Combined corrosion and wear of aluminium alloy 7075-T6. J Bio-and Tribo-Corros 2:9
14. Shanmughasundaram P (2015) Statistical analysis on influence of heat treatment, load and velocity on the dry sliding wear behavior of Aluminium alloy 7075. Mater Phys Mech 22:118–124
15. Ruiz-Andrés M, Conde A, De Damborenea J, García I (2015) Wear behavior of aluminum alloys at slow sliding speeds. Tribol Trans 58:955–962
16. Yang Z-R, Sun Y, Li X-X, Wang S-Q, Mao T-J (2015) Dry sliding wear performance of 7075 Al alloy under different temperatures and load conditions. Rare Met 1–6. https://doi.org/10.1007/s12598-015-0504-7
17. Kumar GV, Rao C, Selvaraj N (2012) Mechanical and dry sliding wear behavior of Al7075 alloy-reinforced with SiC particles. J Compos Mater 46:1201–1209
18. Lakshmipathy J, Kulendran B (2014) Reciprocating wear behaviour of 7075Al/SiC and 6061Al/Al 2 O 3 composites: a study of effect of reinforcement, stroke and load. Tribol Ind 36:117–126
19. Daoud A, El-Khair MA, Abdel-Azim A (2004) Effect of Al2O3 particles on the microstructure and sliding wear of 7075 Al alloy manufactured by squeeze casting method. J Mater Eng Perform 13:135–143
20. Baradeswaran A, Perumal AE (2013) Influence of B 4 C on the tribological and mechanical properties of Al 7075–B 4 C composites. Compos Part B Eng 54:146–152
21. Baskaran S, Anandakrishnan V, Duraiselvam M (2014) Investigations on dry sliding wear behavior of in situ casted AA7075–tic metal matrix composites by using Taguchi technique. Mater Des 60:184–192
22. Wang L, Snidle R, Gu L (2000) Rolling contact silicon nitride bearing technology: a review of recent research. Wear 246:159–173
23. Riley FL (2000) Silicon nitride and related materials. J Am Ceram Soc 83:245–265
24. Xiu Z-Y, Chen G-Q, Wu G-H, Yang W-S, Liu Y-M (2011) Effect of volume fraction on microstructure and mechanical properties of Si3N4/Al composites. Trans Nonferrous Met Soc China 21:285–289
25. Sharma N, Khanna R, Singh G, Kumar V (2016) Fabrication of 6061 aluminum alloy reinforced with Si3N4/n-Gr and its wear performance optimization using integrated RSM-GA. Particul Sci Technol 2016:1–11
26. Suryanarayana RC, Khan S, Koppad PG, Khan Z (2013) Tribological behaviour of hot extruded Al6061-Si3N4 composite. ASME 2013 international mechanical engineering congress and exposition: american society of mechanical engineers. p V02ATA050-V02AT02A
27. Arik H (2008) Effect of mechanical alloying process on mechanical properties of a-Si 3 N 4 reinforced aluminum-based composite materials. Mater Des 29:1856–1861
28. Cambronero L, Sanchez E, Ruiz-Roman J, Ruiz-Prieto J (2003) Mechanical characterisation of AA7015 aluminium alloy reinforced with ceramics. J Mater Process Technol 143: 378–383
29. Kumar NM, Kumaran SS, Kumaraswamidhas L (2016) Aerospace application on Al 2618 with reinforced–Si 3 N 4, AlN and ZrB 2 in-situ composites. J Alloys Compd 672:238–250
30. Hashim J, Looney L, Hashmi M (1999) Metal matrix composites: production by the stir casting method. J Mater Process Technol 92:1–7
31. Sharma P, Sharma S, Khanduja D (2015) Production and some properties of Si 3 N 4 reinforced aluminium alloy composites. J Asian Ceram Soc 3:352–359
32. Shen Y-L, Chawla N (2001) On the correlation between hardness and tensile strength in particle reinforced metal matrix composites. Mater Sci Eng A 297:44–47
33. Hamid AA, Ghosh P, Jain S, Ray S (2008) The influence of porosity and particles content on dry sliding wear of cast in situ Al (Ti)–Al 2 O 3 (TiO 2) composite. Wear 265:14–26
34. Howell G, Ball A (1995) Dry sliding wear of particulate-reinforced aluminium alloys against automobile friction materials. Wear 181:379–390
35. Subramanian C (1992) Some considerations towards the design of a wear resistant aluminium alloy. Wear 155:193–205
36. Mabuchi M, Iwasaki H, Higashi K, Langdon T (1995) Processing and superplastic properties of fine grained Si3N4/Al–Mg–Si composites. Mater Sci Technol 11:1295–300
37. Suresh S, Moorthi NSV, Vettivel S, Selvakumar N (2014) Mechanical behavior and wear prediction of stir cast Al–TiB 2 composites using response surface methodology. Mater Des 59:383–396
38. Sharifi EM, Karimzadeh F, Enayati M (2011) Fabrication and evaluation of mechanical and tribological properties of boron carbide reinforced aluminum matrix nanocomposites. Mater Des 32:3263–3271
39. Sajjadi SA, Ezatpour H, Parizi MT (2012) Comparison of microstructure and mechanical properties of A356 aluminum alloy/Al 2 O 3 composites fabricated by stir and compo-casting processes. Mater Des 34:106–111
40. Rahimian M, Parvin N, Ehsani N (2010) Investigation of particle size and amount of alumina on microstructure and mechanical properties of Al matrix composite made by powder metallurgy. Mater Sci Eng A 527:1031–1038
41. Ramesh C, Khan AA, Ravikumar N, Savanprabhu P (2005) Prediction of wear coefficient of Al6061–TiO 2 composites. Wear 259:602–608
42. Palanivel R, Dinaharan I, Laubscher R, Davim JP (2016) Influence of boron nitride nanoparticles on microstructure and wear behavior of AA6082/tib 2 hybrid aluminum composites synthesized by friction stir processing. Mater Des 106:195–204
43. Venkat Prasat S, Subramanian R, Radhika N, Anandavel B (2011) Dry sliding wear and friction studies on AlSi10Mg–fly ash–graphite hybrid metal matrix composites using Taguchi method. tribology-materials. Surf Interface 5:72–81
44. Archard J (1953) Contact and rubbing of flat surfaces. J Appl Phys 24:981–988
45. Mazahery A, Shabani MO (2012) A comparative study on abrasive wear behavior of semisolid–liquid processed Al–Si matrix

reinforced with coated B4C reinforcement. T Indian I Metals 65:145–154
46. Nuruzzaman DM, Chowdhury MA (2012) Effect of load and sliding velocity on friction coefficient of aluminum sliding against different pin materials. Am J Mater Sci 2:26–31
47. Torabinejad V, Aliofkhazraei M, Sabour Rouhaghdam A, Allahyarzadeh M (2017) Tribological behavior of electrodeposited Ni-Fe multilayer coating. Tribol Trans 60:923–931
48. Hassan AM, Alrashdan A, Hayajneh MT, Mayyas AT (2009) Wear behavior of Al–Mg–Cu–based composites containing SiC particles. Tribol Int 42:1230–1238
49. Zmitrowicz A (2005) Wear debris: a review of properties and constitutive models. J Theor Appl Mech 43:3–35
50. Venkataraman B, Sundararajan G (2000) Correlation between the characteristics of the mechanically mixed layer and wear behaviour of aluminium, Al-7075 alloy and Al-MMCs. Wear 245:22–38
51. Radhika N, Subramaniam R (2013) Wear behaviour of aluminium/alumina/graphite hybrid metal matrix composites using Taguchi's techniques. Ind Lubr Tribol 65:166–174
52. Nguyen Q, Sim Y, Gupta M, Lim C (2015) Tribology characteristics of magnesium alloy AZ31b and its composites. Tribol Int 82:464–471
53. Iwai Y, Honda T, Miyajima T, Iwasaki Y, Surappa M, Xu J (2000) Dry sliding wear behavior of Al 2 O 3 fiber reinforced aluminum composites. Compos Sci Technol 60:1781–1789
54. Lu D, Gu M, Shi Z (1999) Materials transfer and formation of mechanically mixed layer in dry sliding wear of metal matrix composites against steel. Tribol Lett 6:57–61